Electronic Supplementary Material (ESI) for Chemical Science.
This journal is © The Royal Society of Chemistry 2015

# Engineering FRET Strategy to Achieve Ratiometric Two-Photon Fluorescence Response with Large Emission Shift and Its Application to Fluorescence Imaging

**Lin Yuan,*[a] Fangping Jin,[a] Zebing Zeng,*[a] Chengbin Liu,[a] Shenglian Luo[a] and Jishan Wu[b]**

[a] State Key Laboratory of Chemo/Biosensing and Chemometrics, College of Chemistry and Chemical Engineering, Hunan University, Changsha 410082 (PR China)

[b] Department of Chemistry, National University of Singapore, 3 Science Drive 3, 117543, Singapore

E-mail: lyuan@hnu.edu.cn, zbzeng@hnu.edu.cn

# Table of contents

**Materials and instruments.** Unless otherwise stated, all reagents were purchased from commercial suppliers and used without further purification. Solvents used were purified by standard methods prior to use. Twice-distilled water was used throughout all experiments. High resolution mass spectrometric (HRMS) analyses were measured on a Finnigan MAT 95 XP spectrometer. NMR spectra were recorded on an Bruker-300 or 500 spectrometer. Absorption and emission spectra were recorded with a multifunctional microplate reader SpectraMax M5. Cells and tissue imaging was performed with two photon laser scanning microscope (Olympus FV1000 or NOL-LSM 710). TLC analysis was performed on silica gel plates and column chromatography was conducted over silica gel (mesh 200–300), both of which were obtained from the Qingdao Ocean Chemicals.

**Cytotoxicity assays**. HeLa cells were cultured in DMEM supplemented with 10% FBS in an atmosphere of 5% $CO_2$ and 95% air at 37 °C. Before the experiments, the cells were placed in a 96-well plate, followed by addition of increasing concentrations of probe **TR-$H_2S$** (99.9% DMEM and 0.1% DMSO). The final concentrations of the probe were kept from 1 to 15 μM (n = 3). The cells were then incubated at 37 °C in an atmosphere of 5% $CO_2$ and 95% air at 37 °C for 24 h, followed by MTT assays. Untreated assay with DMEM (n = 3) was also conducted under the same conditions.

**Quantum yield calculation**

Quantum yields were determined using rhodamine B (0.70 in MeOH) as a standard according to a published method (Velapoldi, R. A.; Tønnesen, H. H. *J. Fluoresc.* **2004**, *14*, 465). The quantum yield was calculated according to the equation:

$$\Phi_{sample} = \Phi_{standard} \times (A_{standard}F_{sample}/A_{sample}F_{standard})$$

where $\Phi_{sample}$ and $\Phi_{standard}$ are the fluorescence quantum yield of the sample and the standard, respectively; $F_{sample}$ and $F_{standard}$ are the integrated fluorescence intensities of the sample and the standard spectra, respectively; $A_{sample}$ and $A_{standard}$ are the optical densities at the excitation wavelength, of the sample and the standard, respectively.

**Detection limit calculation**

The detection limit was calculated based on the fluorescence titration (Joshi, B. P.; Park, J.; Lee, W. I.; Lee, K. *Talanta*. **2009**, *78*, 903; Wu, M. Y.; Li, K.; Hou, J. T.; Huang, Z.; Yu, X. Q. *Org. Biomol. Chem.* **2012**, *10*, 8342). To determine the S/N ratio, the emission intensity of **TR-$H_2S$** without $Na_2S$ was measured by 20 times and the standard deviation of blank measurements was determined. Under the present conditions, a good linear relationship between the emission ratios ($I_{500}/I_{625}$) and the $H_2S$ concentration could be obtained in the 1-80 μM (R = 0.994), as shown in Figure S5. The detection limit is then calculated with the equation: detection limit = 3σ/m, where σ is the standard deviation of blank measurements, m is the slope between the emission ratios versus sample concentration. The detection limit was measured to be 0.3 μM at S/N = 3 (signal-to-noise ratio of 3:1).

**HeLa cells culture and imaging using probe TR-$H_2S$.** HeLa cells were grown in Dulbecco's modified Eagle's medium (DMEM) supplemented with 10% FBS (fetal bovine serum) in an atmosphere of 5% $CO_2$ and 95% air at 37 °C. The cells were placed on 1-well plates and allowed to adhere for 24 h. Immediately before the experiments, the cells were washed with PBS buffer, and then the cells were incubated with probe **TR-$H_2S$** (5 μM) for 30 min at 37 °C, or were pre-incubated

with probe **TR-$H_2S$** (5 μM) for 30 min and then further treated with $Na_2S$ (100 μM) for 30 min at 37 $^oC$. Subsequently, the cells were washed in PBS medium. The fluorescence images were acquired through a con-focal laser scanning microscopy.

**Preparation of fresh mouse liver slices and two-photon fluorescence imaging.** Slices were prepared from the liver of two weeks old mice. Slices were cut to 400 μm thickness by using a vibrating-blade microtome in 15 mM PBS (pH 7.4). Slices were incubated with probe **TR-$H_2S$** (5 μM) for 30 min at 37 $^oC$ or pretreated with of **TR-$H_2S$** (5 μM) for 30 min and then further treated with $Na_2S$ (100 μM) for 30 min at 37 $^oC$. Slices were then washed three times with PBS, transferred to glass-bottomed dishes, and observed under a two-photon con-focal microscopy.

**Synthesis**

Compound **1** was prepared by the literature method (M. Y. Kang, C. S. Lim, H. S. Kim, E. W. Seo, H. M. Kim, O. Kwon, B. R. Cho, *Chem. Eur. J*. **2012**, *18*, 1953-1960), and the synthesis of the other compounds is described below.

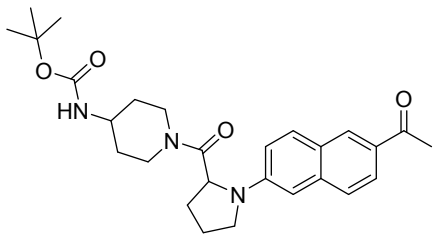


**Synthesis of compound 2**: A mixture of compound **1** (142 mg, 0.5 mmol), 4-(*N*-Boc-amino)piperidine (100 mg, 0.5 mmol), EDC·HCl (154 mg, 0.6 mmol), and HOBt (124 mg, 1.7 mmol) in $CH_2Cl_2$ (5 mL) was stirred at room temperature for overnight under a nitrogen atmosphere. The resulting mixture was extracted with saturated $NaHCO_3$, dried over anhydrous $Na_2SO_4$, filtered,

and concentrated under reduced pressure. The crude product was purified by column chromatography on silica gel ($CH_2Cl_2$ to $CH_2Cl_2$/MeOH = 50:1) to give compound **2** in 76% yield (177 mg). $^1$H NMR (500 MHz, $CDCl_3$): δ 8.29 (s, 1H), 7.91 (dd, *J* = 8.7, 1.5 Hz, 1H), 7.77 (d, *J* = 9.0 Hz, 1H), 7.58 (dd, *J* = 15.2, 8.7 Hz, 1H), 6.87 (d, *J* = 8.8 Hz, 1H), 6.66 (d, *J* = 4.5 Hz, 1H), 4.70 (s, 1H), 4.53 – 4.48 (m, 1H), 4.04 (d, *J* = 12.4 Hz, 1H), 3.77 (s, 2H), 3.59 (s, 1H), 3.29 (dt, *J* = 12.3 Hz, 1H), 2.84 (dt, *J* = 10.1 Hz, 1H), 2.66 (d, *J* = 10.2 Hz, 3H), 2.37 (dd, *J* = 9.1 Hz, 1H), 2.08 (m, 11.5 Hz, 5H), 1.77 (s, 1H), 1.48 (9H), 1.28 (s, 1H); $^{13}$C NMR (126 MHz, $CDCl_3$): δ 197.74, 170.68, 155.05, 146.72, 137.75, 131.02, 130.54, 126.02, 125.23, 124.55, 116.05, 105.17, 79.74, 59.34, 58.94, 48.64, 43.89, 41.33, 33.45, 33.12, 32.40, 30.82, 30.50, 28.41, 26.38, 23.67, 23.55. MS ($ESI^+$) 466.3 ($M + H^+$); HRMS (EI): $(M)^+$ calcd. for $C_{27}H_{35}N_3O_4$, 465.2628; found, 465.2619.

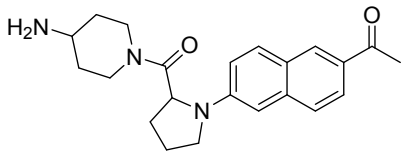


**Synthesis of compound 3**: Compound **2** (349 mg, 0.75 mmol) was dissolved in $CH_2Cl_2$ (2 mL), then $CF_3COOH$ (2 mL) was added, the mixture was stirred at room temperature for 30 min under a nitrogen atmosphere. The resulting mixture was concentrated under reduced pressure. The crude product was purified by column chromatography on silica gel ($CH_2Cl_2$/MeOH = 100: 1 to 20: 1) to give compound **3** in 92% yield (252 mg). $^1$H NMR (500 MHz, DMSO): δ 8.42 (s, 1H), 8.10 (d, *2*H, -N*H*$_2$), 7.87 (d, *J* = 8.9 Hz, 1H), 7.82 (d, *J* = 8.6 Hz, 1H), 7.64 (t, *J* = 8.7 Hz, 1H), 6.92 (dd, *J* = 8.6 Hz, 1H), 6.67 (d, *J* = 11.8 Hz, 1H), 4.98 (dd, 7.9 Hz, 1H), 4.36 (t, *J* = 12.4 Hz, 1H), 4.23 (t, *J* = 12.7 Hz, 1H), 3.55 (dd, *J* = 10.5, 6.0 Hz, 2H), 3.22 – 3.10 (m, 1H), 2.78 – 2.64 (m, 1H), 2.62 (s, 3H),

2.42 – 2.27 (m, 1H), 1.98 (m, 5H), 1.61 (m, 1H), 1.45 – 1.30 (m, 1H), 1.24 (s, 1H); $^{13}$C NMR (126 MHz, DMSO) δ 197.34, 170.29, 147.34, 137.70, 131.08, 130.23, 126.09, 124.47, 116.99, 104.92, 58.43, 58.30, 48.72, 48.13, 47.86, 43.19, 31.14, 30.75, 30.51, 30.35, 29.80, 29.45, 26.81, 23.58, 23.49. MS (ESI$^+$) 366.3 (M + H$^+$); HRMS (EI): (M)$^+$ calcd. for $C_{22}H_{27}N_3O_2$, 365.2103; found, 365.2112.

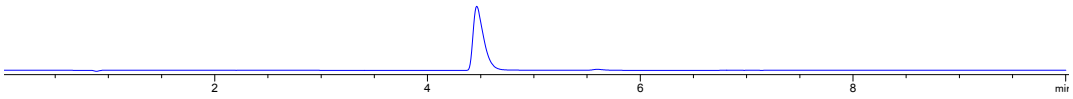


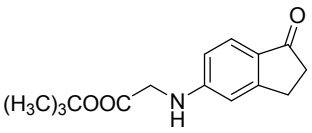


**Synthesis of compound 5**: A mixture of compound **4** (191 mg, 1.3 mmol), tert-Butyl bromoacetate (305 mg, 1.6 mmol), $K_2CO_3$ (215 mg, 1.6 mmol), NaI (61 mg, 0.4 mmol) in MeCN (150 mL) was refluxed under nitrogen atmosphere for 18 h. The product was extracted with ethyl acetate, washed with brine, and purified by flash column chromatography on silica gel ($CH_2Cl_2$ to $CH_2Cl_2$/MeOH = 60: 1) to give compound **5** in 52% yield (176 mg). $^1$H NMR (300 MHz, $CDCl_3$): δ 7.64 (d, *J* = 8.4 Hz, 1H), 6.60 (dd, *J* = 8.4, 2.1 Hz, 1H), 6.52 (s, 1H), 3.90 (s, 2H), 3.09 – 2.99 (m, 2H), 2.70 – 2.60 (m, 2H), 1.54 (s, 9H); $^{13}$C NMR (75 MHz, $CDCl_3$) δ 204.76, 169.15, 158.40, 152.50, 127.51, 125.47, 113.41, 107.22, 82.62, 45.62, 36.26, 27.99, 25.71. MS (ESI$^+$) 262.1 (M + H$^+$); HRMS (EI): (M)$^+$ calcd. for $C_{15}H_{19}NO_3$, 261.1365; found, 261.1372.

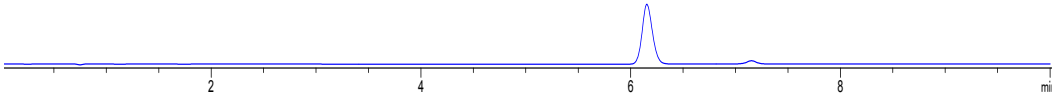


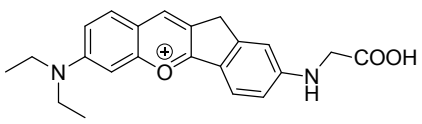

**Synthesis of compound 6**: 4-(diethylamino)salicylaldehyde (193 mg, 1 mmol) and compound **5** (260 mg, 1 mmol) were dissolved in $MeSO_3H$ (2 mL) and stirred at 90 °C for 2 h. After cooling to room temperature, the mixture was added to ice-water solution (30 g), then 70% perchloric acid (0.5 mL) was added. The resulting mixture was extracted with $CH_2Cl_2$ (6 × 30 mL), dried over anhydrous $Na_2SO_4$, filtered, and concentrated under reduced pressure. The crude product was purified by column chromatography on silica gel ($CH_2Cl_2$/MeOH = 50: 1 to 10: 1) to give compound **6** in 63% yield (292 mg). $^1$H NMR (300 MHz, MeOD): δ 8.18 (s, 1H), 8.86 (d, *J* = 8.6 Hz, 1H), 7.71 (d, *J* = 8.6 Hz, 1H), 7.13 (dd, *J* = 6.4 Hz, 1H), 7.05 (d, *J* = 2.4 Hz, 1H), 6.92 (dd, *J* = 8.7 Hz, 1H), 6.84 (d, *J* = 2.0 Hz, 1H), 3.90 (4H), 3.67 (q, *J* = 6.9 Hz, 4H), 1.37 (7, *J* = 6.9 Hz, 4H); $^{13}$C NMR (75 MHz, MeOD) δ 171.31, 156.60, 157.27, 153.23, 153.12, 140.75, 139.95, 134.57, 130.76, 126.68, 124.02, 119.51, 115.03, 113.73, 113.48, 96.49, 45.12, 44.99, 13.05. MS (ESI$^+$) 363.2 ($M^+$); HRMS (ESI): $(M)^+$ calcd. for $C_{22}H_{23}N_2O_3^+$, 363.1709; found, 363.1725.

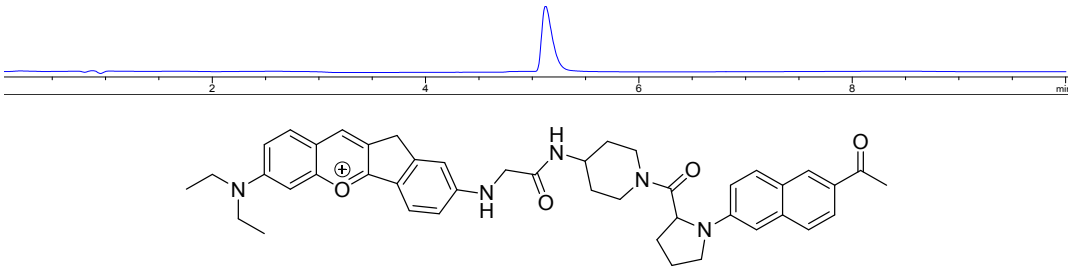

**Synthesis of compound TR-$H_2S$**: A mixture of compound **3** (51 mg, 0.11 mmol), **6** (40 mg, 0.11 mmol), EDC·HCl (25 mg, 0.13 mmol), and HOBt (21 mg, 0.13 mmol) in $CH_2Cl_2$ (3 mL) was stirred at room temperature for overnight under a nitrogen atmosphere. The resulting mixture was extracted with saturated $NaHCO_3$, dried over anhydrous $Na_2SO_4$, filtered, and concentrated under reduced pressure. The crude product was purified by column chromatography on silica gel ($CH_2Cl_2$ to $CH_2Cl_2$/MeOH = 20: 1) to give compound **TR-$H_2S$** in 74% yield (690 mg). $^1$H NMR (300 MHz, $CDCl_3$) δ 8.83 (1H), 8.59 (N*H*, 1H), 8.26-8.19 (d, *J* = 2.8 Hz, 1H), 7.94-7.70 (3H), 7.56-7.33 (2H),

7.16-7.03 (2H), 6.95-6.92 (d, $J$ = 1.0 Hz, 1H), 6.83-6.72 (2H), 6.61-6.59 (d, $J$ = 1.0 Hz, 1H), 4.67 (s, 1H), 4.27-4.10 (5H), 3.82-3.54 (9H), 3.32-3.09 (m, 1H), 2.62 (s, 1H), 2.25-1.80 (8H), 1.32, (t, $J$ = 8.4 Hz, 6H); $^{13}$C NMR (126 MHz, $CDCl_3$) δ 197.73, 171.40, 170.42, 168.73, 156.36, 156.35, 152.81, 146.77, 146.74, 138.37, 138.12, 137.73, 131.15, 130.94, 130.92, 130.48, 126.86, 126.04, 126.01, 125.91, 124.97, 124.33, 124.24, 119.93, 116.14, 113.67, 113.21, 104.92, 97.03, 58.82, 58.69, 48.55, 48.48, 45.43, 43.64, 40.53, 40.45, 32.55, 31.87, 29.65, 29.27, 26.39, 23.48, 12.42. MS ($M^+$) 710.3; HRMS (ESI): $(M)^+$ calcd. for $C_{44}H_{48}N_5O_4^+$, 710.3706; found, 710.3715.

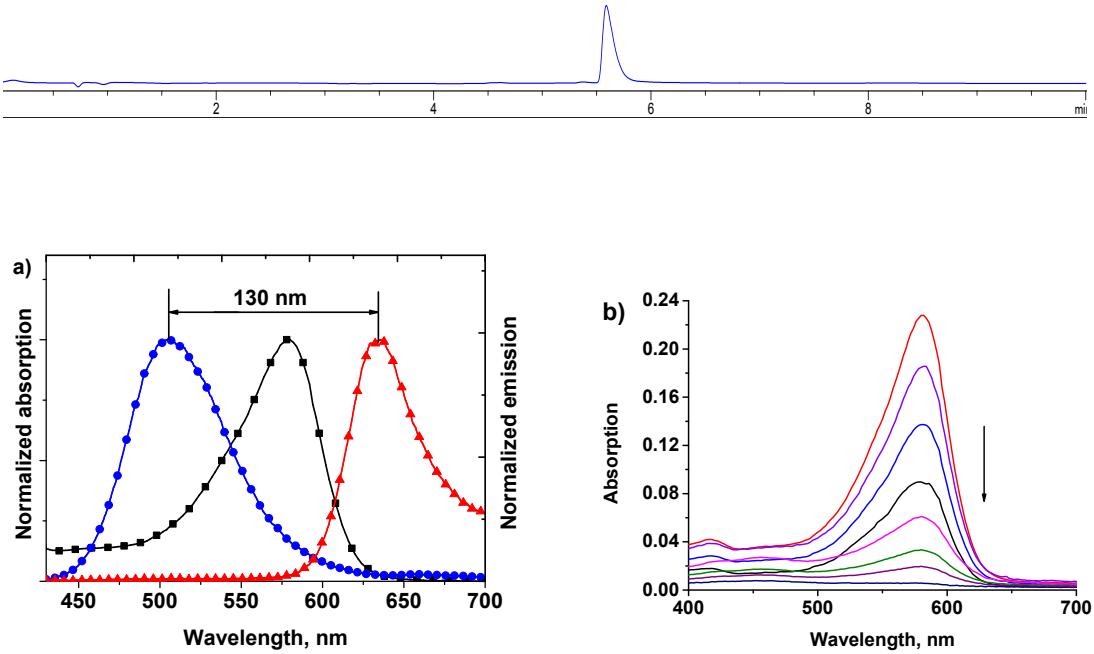


**Fig. S1**. (a) Normalized TPE emission spectrum of **2** (●), **6** (▲), and absorption spectrum **6** (■) at 25 °C. (b) Absorption spectrum of **6** upon titration of $H_2S$ ($Na_2S$, 0-50 μM) in a PBS (pH = 7.4, 1% DMSO, 1 mg/mL HSA).

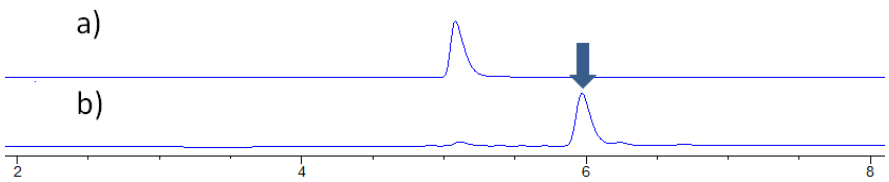

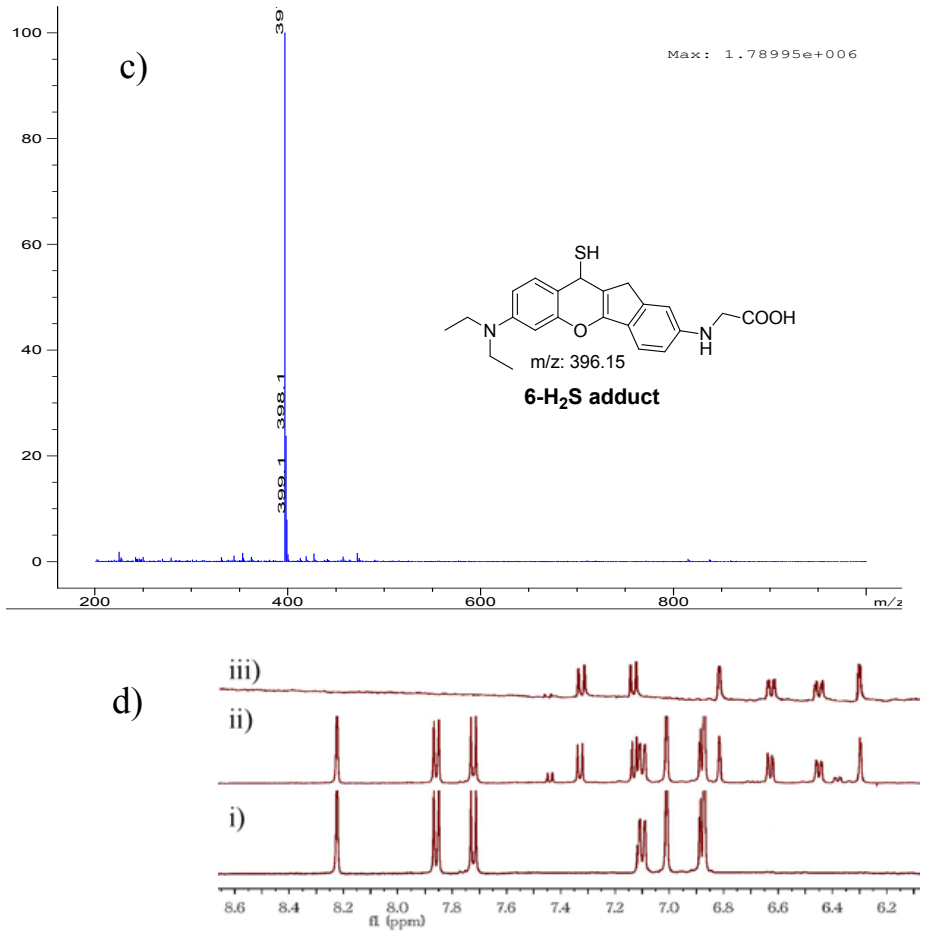


**Fig. S2**. Reversed-phase HPLC chromatograms with absorption (350 nm) detection. Assigned peaks were confirmed by $ESI^+$. The arrow indicates adduct product of compound **6** with $Na_2S$. (a) An authentic solution of 100 μM compound **6**. (b) A sample solution of 100 μM compound **6** in the presence of 200 μM $Na_2S$ for 1 min. (c) The MS of 100 μM compound **6** in the presence of 200 μM $Na_2S$ for 1 min. (d) $^1H$ NMR spectra of **6** (500 MHz) in the absence (i) and presence of 0.5 equiv. (ii) and 2equiv. (iii) $Na_2S$ in DMSO-$d_6$/$D_2O$ (8:2, v/v).

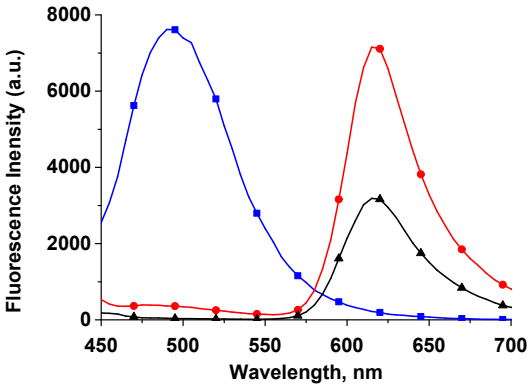


**Fig. S3**. One-photon ($\lambda_{ex}$ = 378 nm) induced emission spectra of **TR-$H_2S$** (●), **2** (■), and **6** (▲) at 25°C in MeOH. Emission at around 500 nm is quenched (>97%) upon excitation of **TR-$H_2S$** at 378 nm compared to excitation of **2** at 378 nm.

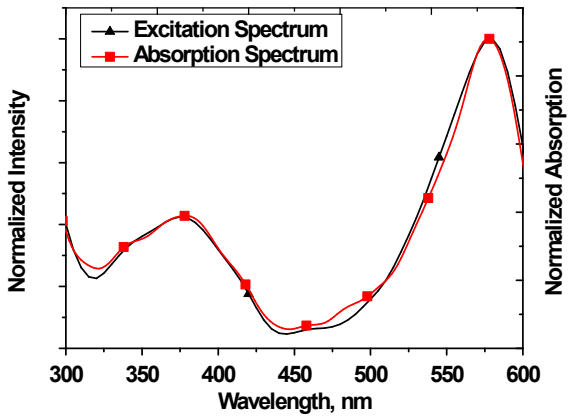


**Fig. S4**. The normalized absorption spectrum (■) and excitation spectrum (▲) of **TR-$H_2S$**, both normalized to 1 at the **TR-$H_2S$** absorption peak (~570 nm).

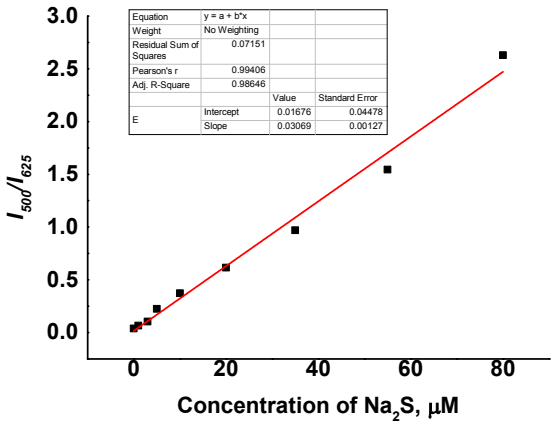


**Fig. S5**. The intensity ratio ($I_{500}/I_{625}$) of **TR-$H_2S$** versus the concentration of $Na_2S$ changes from 1 to 80 μM.

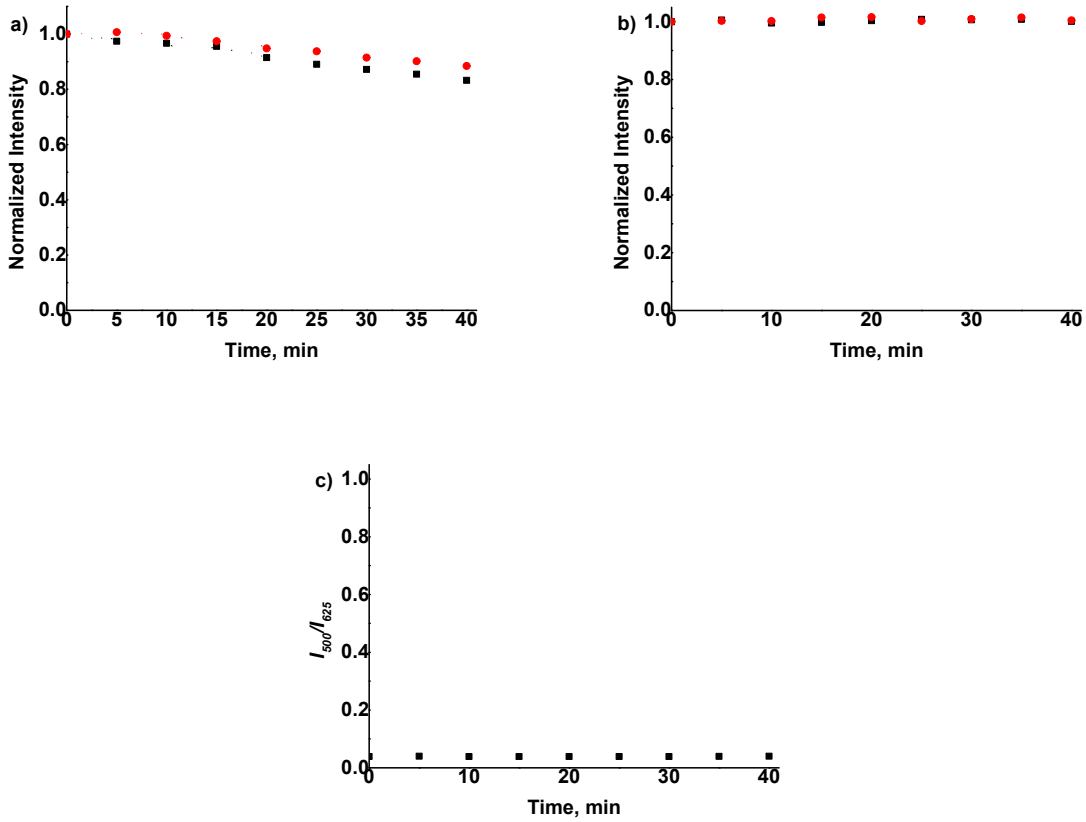


**Fig. S6**. The normalized fluorescence intensity of dye **2** (●), and **6** (■) exposure to UV light (80 W, 365 nm) (a) or femtosecond laser (80 W, 760 nm) for 0-40 min. (c) The intensity ratio ($I_{500}/I_{625}$) of **TR-$H_2S$** exposure to femtosecond laser (80 W, 760 nm) for 0-40 min

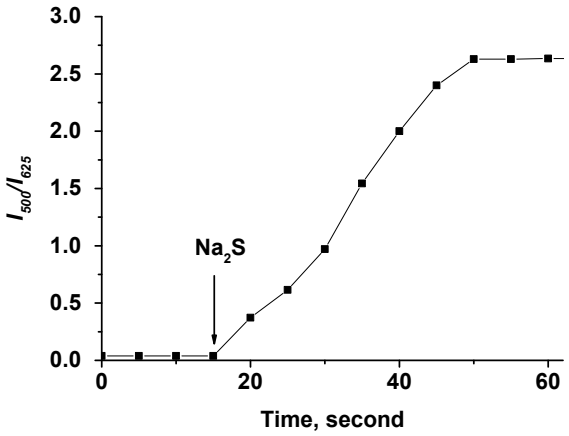


**Fig. S7**. The intensity ratio ($I_{500}/I_{625}$) changes with times of **TR-$H_2S$** in the absence (0-15 s) and presence (20-60 s) of $Na_2S$ (80 μM).

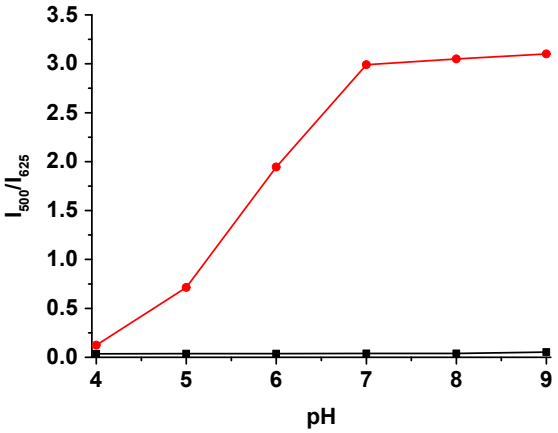


**Fig. S8**. Fluorescence intensity ratios ($I_{500}/I_{625}$) of probe **TR-$H_2S$** in the absence (■) or presence (●) of $H_2S$ (100 μM) at different pH.

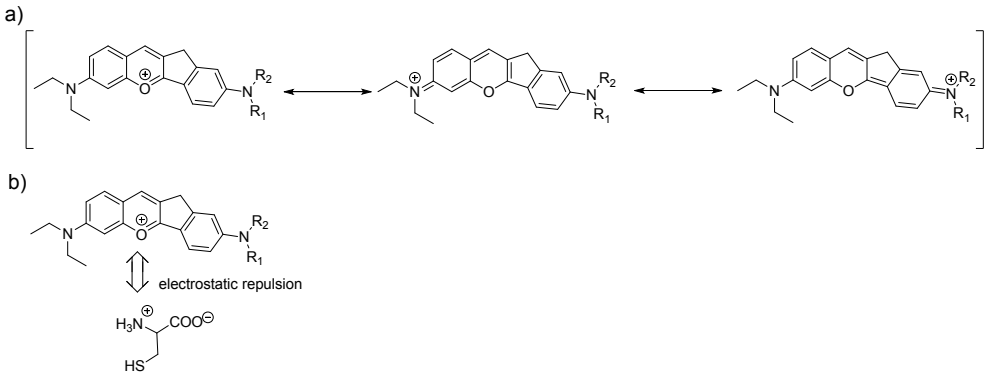


**Fig. S9**. Resonance structures of the cationic anthocyanidin analogues. B) The proposed electrostatic repulsion interaction between the cationic anthocyanidin analogues and the cationic ammonium group of Cys.

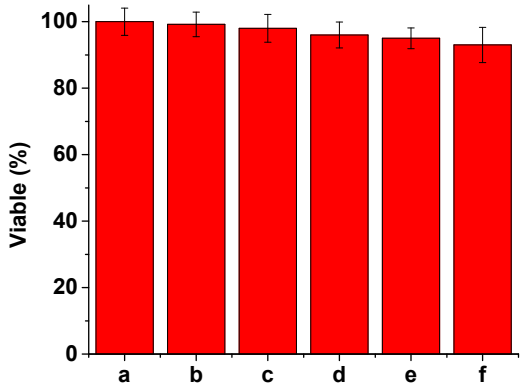


**Fig. S10**. Percentage of viable HeLa cells after treatment with indicated concentrations (a: 0 μM; b: 1 μM; c: 2 μM; d: 5 μM; e: 10 μM; f: 15 μM) of probe **TR-$H_2S$** after 24 hours by MTT assay.

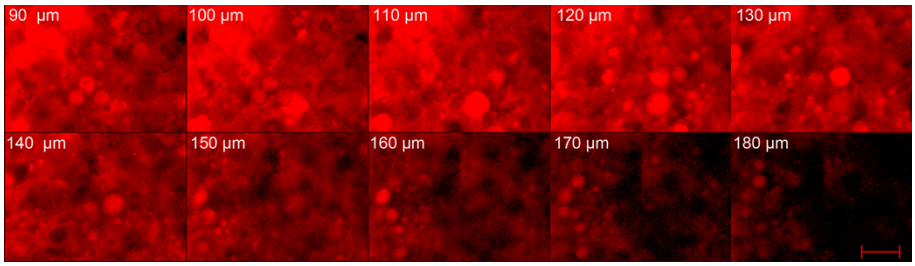


**Fig. S11**. Depth fluorescence images of liver slice incubated with **TR-$H_2S$** (5 μM) for 30 min, emission measured at 591-704 nm. Scale bars: 20 μm

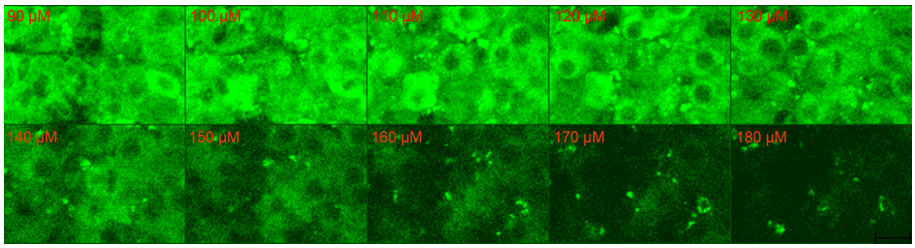


**Fig. S12**. Depth fluorescence images of liver slice incubated with **TR-$H_2S$** (5 μM) for 30 min and then further incubated with $Na_2S$ (100 μM) for another 30 min, emission measured at 471-560 nm. Scale bars: 20 μm

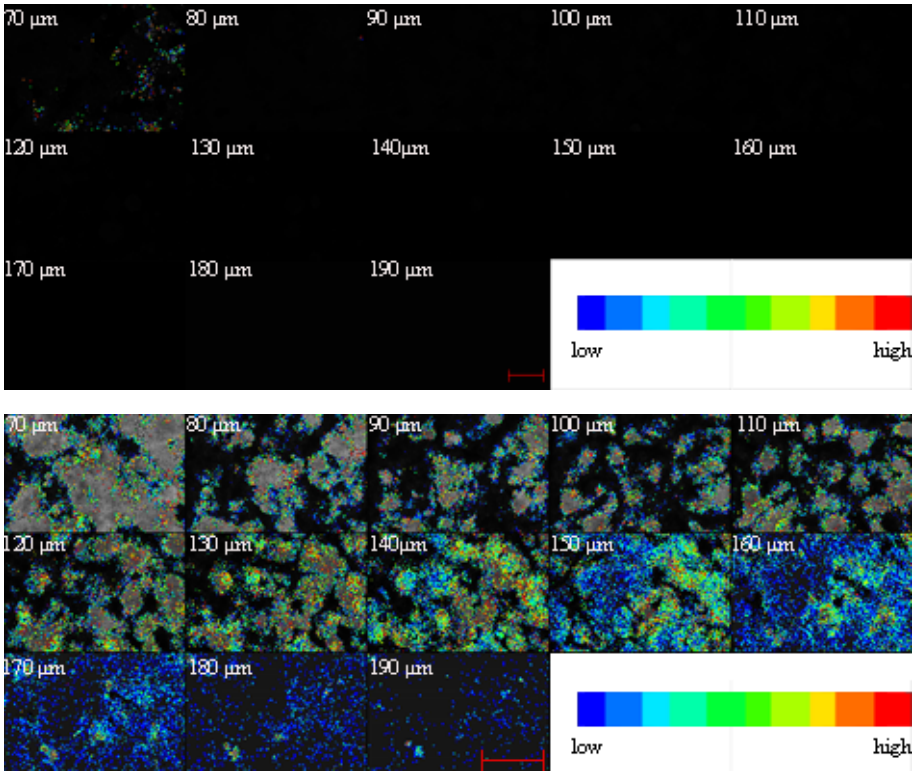


**Fig. S13**. (top) Ratio ($F_{green}/F_{red}$) images of liver slice incubated with **TR-$H_2S$** (5 μM) for 30 min. (bottom) Ratio ($F_{green}/F_{red}$) images of liver slice incubated with **TR-$H_2S$** (5 μM) for 30 min and then further incubated with $Na_2S$ (100 μM) for another 30 min. The emission measured at 471-560 nm for green channel and 591-704 nm for red channel, respectively. Scale bars: 20 μm.

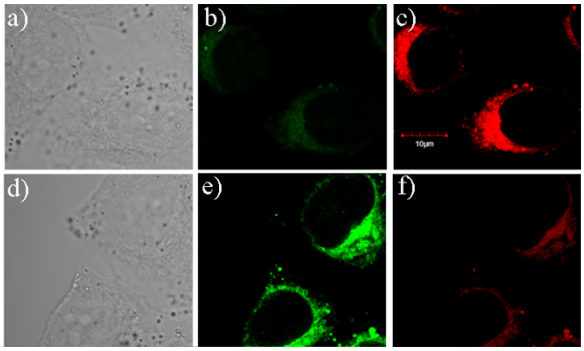


**Fig. S14**. Imaging of HeLa cells. a-c) Cell incubated with **TR-$H_2S$** (5 μM) for 30 min, emission measured at 471-560 nm (b) and 591-704 nm (c); d-f) Cell incubated with **TR-$H_2S$** (5 μM) for 30 min and then further incubated with $Na_2S$ (100 μM) for another 30 min, emission measured at 471-560 nm (e) and 591-704 nm (f). Scale bars: 10 μm.

**Table S1.** Properties of ratiometric fluorescent $H_2S$ probes

| Probes | $\lambda_{ex}$/nm (OP/TP)[a] | $\Delta\lambda_{em}$/nm [b] | detection limit/μM | Solution | Mechanism | Application |
|---|---|---|---|---|---|---|
| CyN3 [1] | 625/-- | 40 | 0.08 | HEPES (pH=7.4, 40 mM) | ICT | macrophage cells |
| AHS-1/2 [2] | 400/800 | 62 | 0.05 | EtOH/PBS (v/v1:4, pH 7.0) | ICT | MCF-7 cells |
| CouMC [3] | 475/-- | 140 [c] | 1 | PBS (20 mM, pH 7.40, 2% DMSO, v/v) | ICT | MCF-7 cells |
| nitroolefin-based coumarin 2[4] | 467/-- | 139 [c] | 2.5 | DMF | ICT | -- |
| SHS-M2 [5] | 373/750 | 81 | 0.4 | HEPES (30 mM, 100 mM KCl, pH 7.4) | ICT | HeLa cells Brain slices |
| RHP-2 [6] | 415/-- | 67 | 0.27 | PBS buffer (20 mM, pH 7.4, 5%$CH_3CN$) | ICT | MCF-7 cells |
| NAP-1 [7] | 415/-- | 67 | 0.11 | PBS buffer (20 mM, pH = 7.4, 5% $CH_3CN$) | ICT | MCF-7 cells |
| Azido-Cresyl violet[8] | 535/-- | 54 | 0.1 | phosphate buffer (60 mM, pH 7.4). | ICT | MCF-7 cells zebrafish. |
| Flavylium derivative[9] | 450/-- | 205 [c] | 0.14 | PBS buffer (10 mM, pH 7.4, 30% $CH_3CN$ | ICT | HeLa cells |
| HS–Cy[10] | 700-510/-- | 155 [c] | 0.01 | HEPES buffer (20 mM, pH 7.4, 0.5% $CH_3CN$) | ICT | HepG2 cells |
| Azido-HBT[11] | 330/-- | 95 [d] | 2.4 | PBS (50 mM, pH 7.4,30% $CH_3CN$). | ESIPT | HeLa cells |
| 3-(disulfanyl)-propionic acid-caged HMBT [12] | 320/-- | 104 [d] | 0.068 | Tris-HCl (10 mM, pH 7.40) | ESIPT | HeLa cells |
| E1 [13] | 295/-- | 131 [d] | 0.12 | Tris-HCl buffer (20 mM, pH 7.4, 40% EtOH) | ESIPT | HeLa cells |
| FBBP[14] | 310/-- | 103 [d] | 0.51 | $CH_3CN$ : $H_2O$ (v/v = 2 : 8, pH 7.5) | ESIPT | yeast cell |
| SR400 [15] | 400/-- | 60 | --- | PBS buffer (20 mM, pH 7.4) | FRET | HEK293 |
| SR550 [15] | 550/-- | 90 | --- | PBS buffer (20 mM, pH 7.4) | FRET | --- |
| TR-$H_2S$[16] | 378/760 | 125 [e] | 0.3 μM | PBS (pH = 7.4, 2% DMSO, 1 mg/mL HSA) | FRET | HeLa cells Liver slice |

[a] One-photon (OP) excitation wavelength and two-photon (TP) excitation wavelength. [b] The emission shift between two peaks before and after interaction with $H_2S$. [c] Although these probes based on ICT mechanism have large emission shift, their maximum excitation/absorption wavelengths are also remarkably fluctuated/shifted before and after reaction with $H_2S$; thus, these probes have to irradiate at the excitation maxima of either absorbance band or the iso-excitation point (absorptivity of these probes at this point is quite weak.). Therefore as a result, one band of fluorescence brightness is sacrificed or both bands of fluorescence are equally sacrificed,

which are not conducive to image purpose. One extreme example is HS–Cy[10], which has to excite at two different absorption bands due to the large excitation shift (190 nm) before and after reaction with $H_2S$. [d] These probes based on ESIPT (excited state intramolecular proton transfer) mechanism also display large emission shift, but the short excitation wavelengths in the UV range (295-330 nm) typically used for this type of probes could perturb the cells. In addition, the short excitation wavelength leads to two emission bands, among which one emission band also lies in the UV range (356-374 nm), thus it is not desirable for imaging purpose. [e] Probe **TR-$H_2S$** collectively displays several unique advantages, such as its large emission shift (125 nm), unchanged maximum low energy TPE wavelength (760 nm) and both emission bands located at long wavelength region (500-630 nm).

## References


1. F. Yu, P. Li, P. Song, B. Wang, J. Zhao and K. Han, *Chem. Commun.*, 2012, **48**, 2852-2854.
2. X. L. Liu, X. J. Du, C. G. Dai and Q. H. Song, *J. Org. Chem.*, 2014, **79**, 9481-9489.
3. Y. Chen, C. Zhu, Z. Yang, J. Chen, Y. He, Y. Jiao, W. He, L. Qiu, J. Cen and Z. Guo, *Angew. Chem. Int. Ed.*, 2013, **52**, 1688-1691.
4. M. Y. Wu, K. Li, J. T. Hou, Z. Huang and X. Q. Yu, *Org. Biomol. Chem.*, 2012, **10**, 8342-8347.
5. S. K. Bae, C. H. Heo, D. J. Choi, D. Sen, E. H. Joe, B. R. Cho and H. M. Kim, *J. Am. Chem. Soc.*, 2013, **135**, 9915-9923.
6. L. Zhang, W. Q. Meng, L. Lu, Y. S. Xue, C. Li, F. Zou, Y. Liu and J. Zhao, *Sci. Rep.*, 2014, **4**.
7. L. Zhang, S. Li, M. Hong, Y. Q. Xu, S. S. Wang, Y. Liu, Y. Qian and J. Zhao, *Org. Biomol. Chem.*, 2014, **12**, 5115-5125.
8. Q. Q. Wan, Y. C. Song, Z. Li, X. H. Gao and H. M. Ma, *Chem. Commun.*, 2013, **49**, 502-504.
9. J. Liu, Y. Q. Sun, J. Zhang, T. Yang, J. Cao, L. Zhang and W. Guo, *Chem. -Eur. J.*, 2013, **19**, 4717-4722.
10. J. S. Xu Wang, W. Zhang, X. Ma, J. Lv and B. Tang, *Chem. Sci.*, 2013, **4**, 2551-2556.
11. Y. Jiang, Q. Wu and X. Chang, *Talanta*, 2014, **121**, 122-126.
12. Q. Huang, X. F. Yang and H. Li, *Dyes. Pigment.*, 2013, **99**, 871-877.
13. Z. Xu, L. Xu, J. Zhou, Y. Xu, W. Zhu and X. Qian, *Chem. Commun.*, 2012, **48**, 10871-10873.
14. S. Goswami, A. Manna, M. Mondal and D. Sarkar, *Rsc. Adv.*, 2014, **4**, 62639-62643.
15. L. Wei, L. Yi, F. Song, C. Wei, B. F. Wang and Z. Xi, *Sci. Rep.*, 2014, **4**.
16. This work.

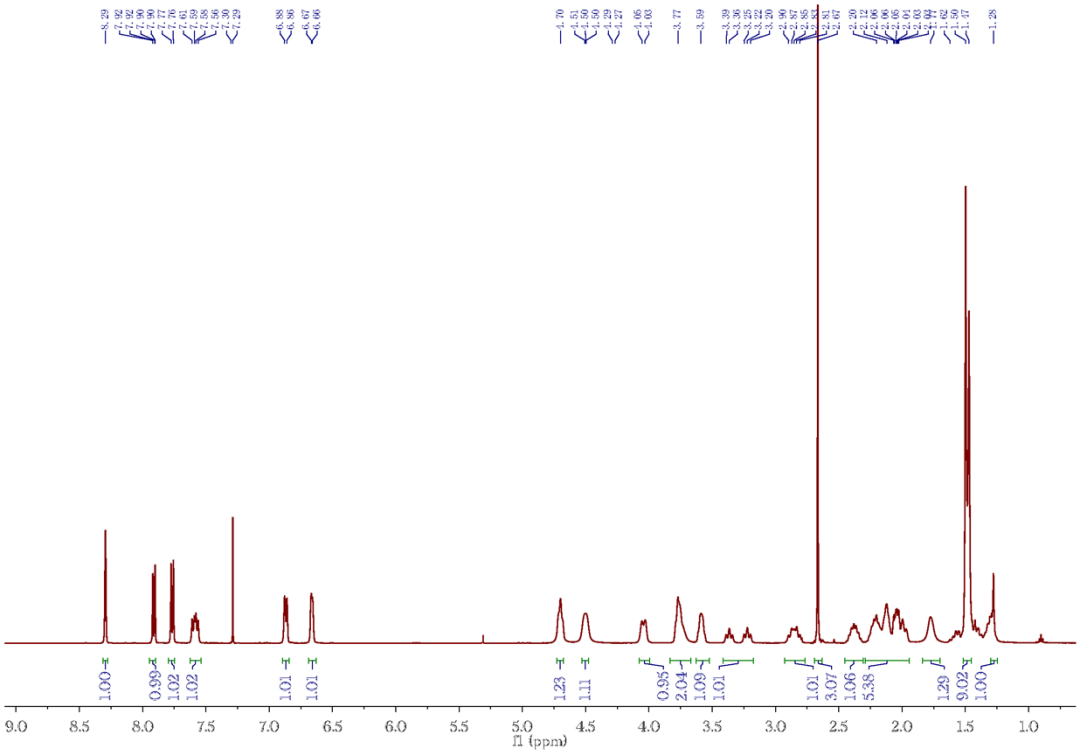

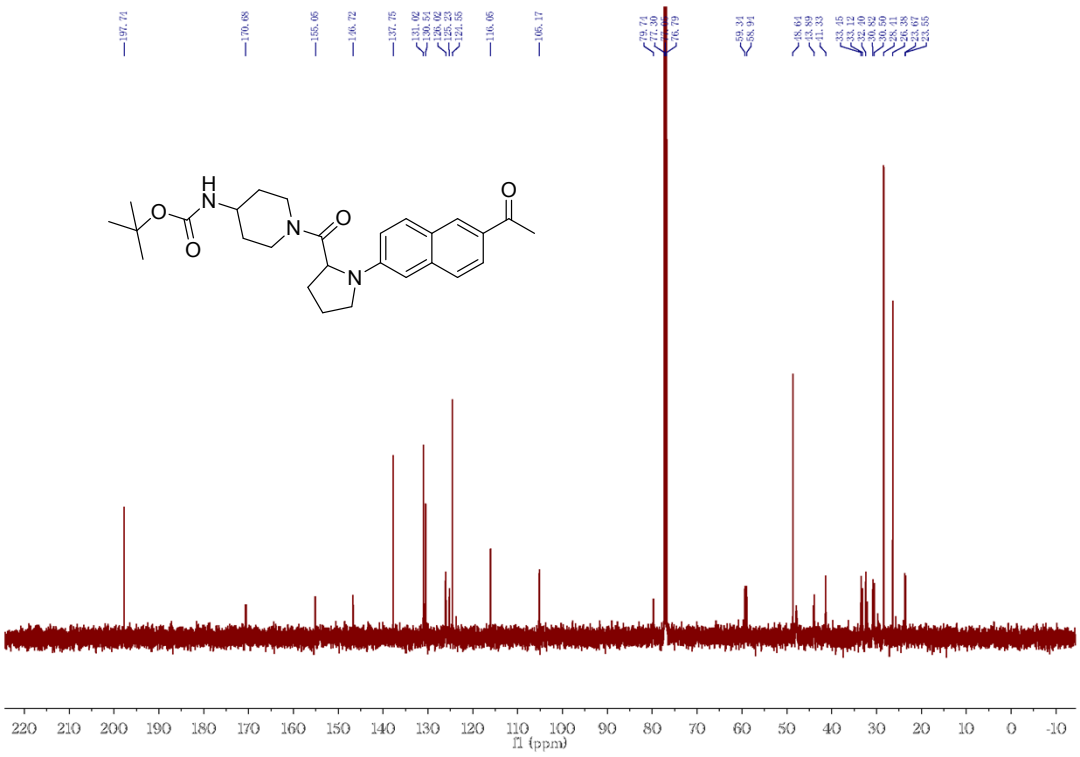

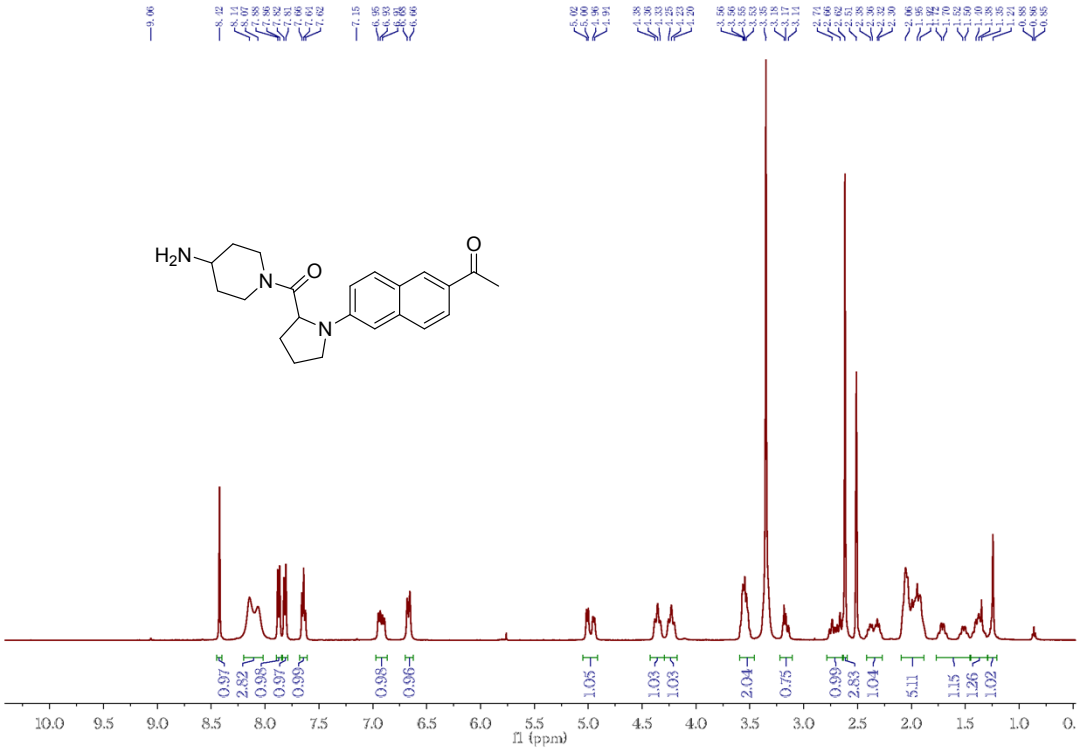
H2N
O
N
O
N
O
f1 (ppm)

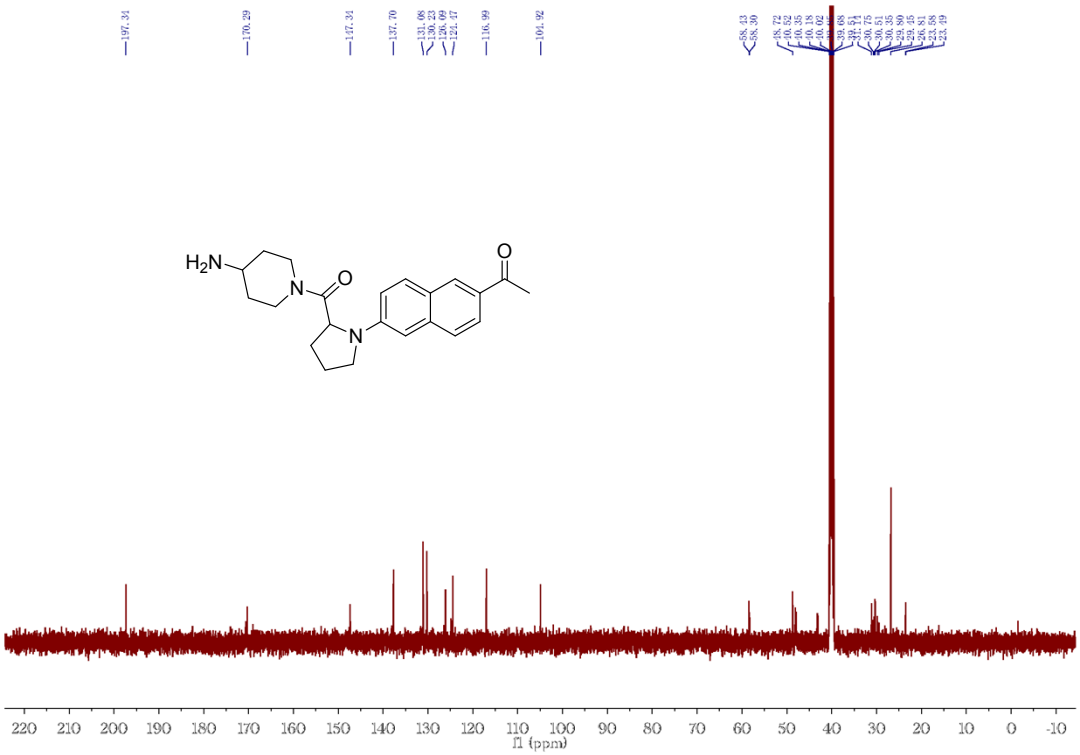
H2N
O
N
O
N
O
f1 (ppm)

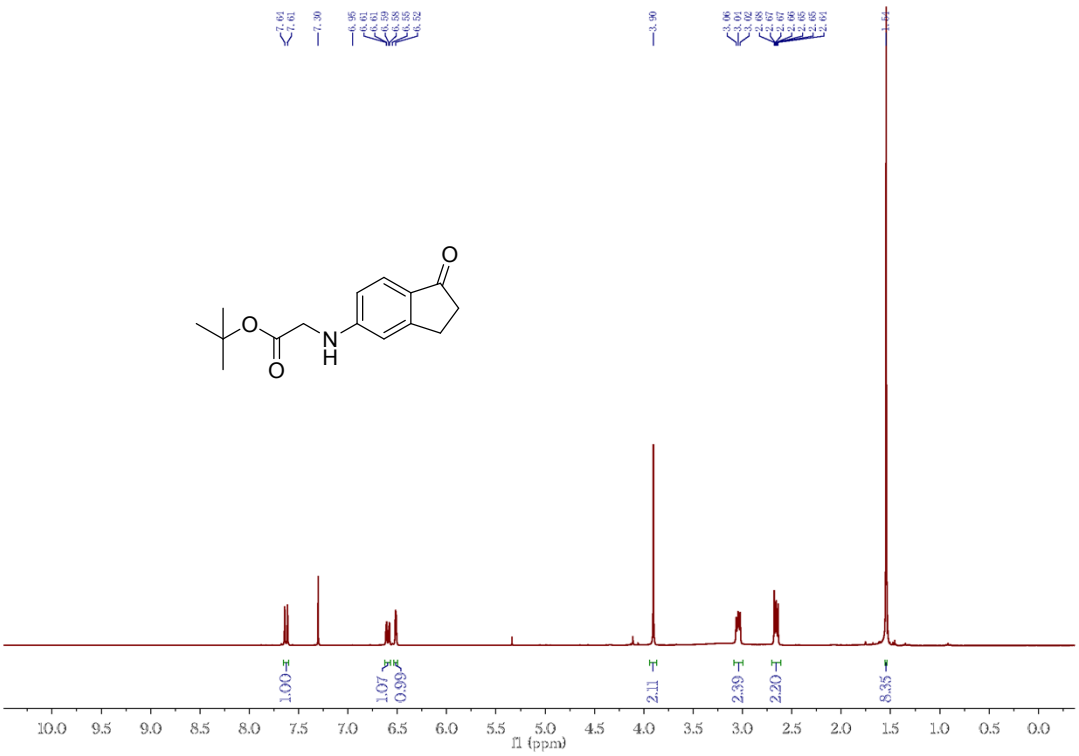
7.64
7.61
7.30
6.95
6.61
6.59
6.58
6.55
6.52
3.90
3.06
3.04
3.02
2.69
2.67
2.67
2.66
2.65
2.64
2.61
1.64
1.00
1.07
0.99
2.11
2.39
2.20
8.35
10.0 9.5 9.0 8.5 8.0 7.5 7.0 6.5 6.0 5.5 5.0 4.5 4.0 3.5 3.0 2.5 2.0 1.5 1.0 0.5 0.0
f1 (ppm)
O
O
N
H
O
O

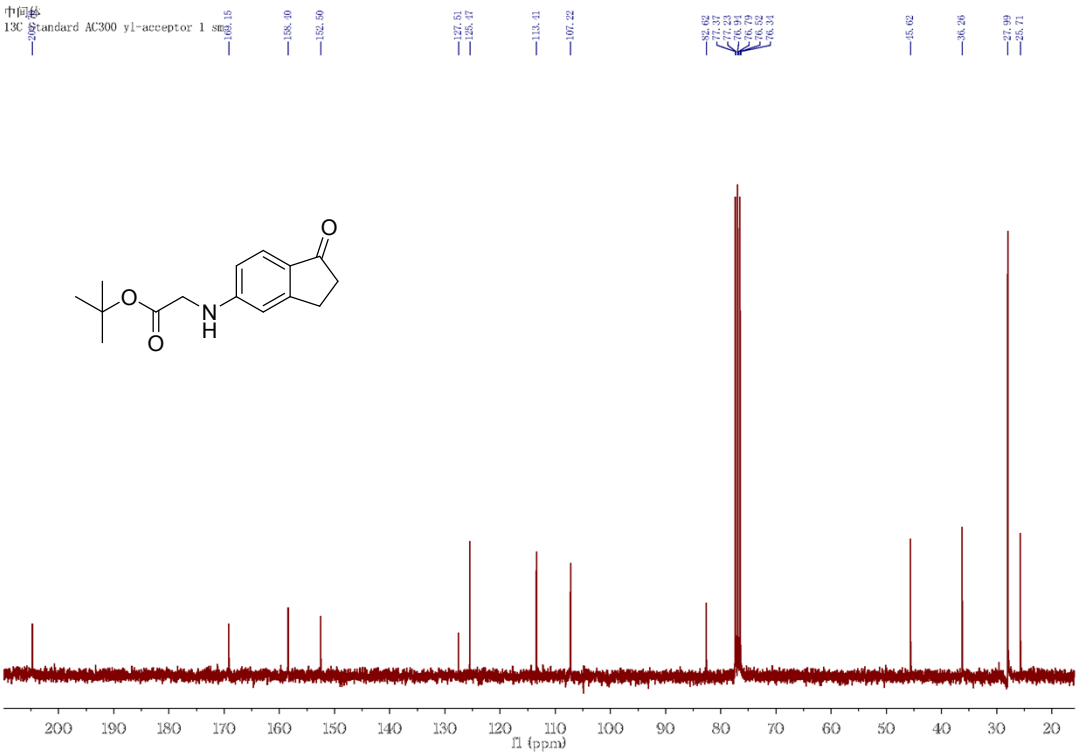
中间体
13C standard AC300 yl-acceptor 1 sm
169.15
158.90
152.59
127.51
125.47
113.41
107.22
82.62
77.23
77.00
76.79
76.52
76.34
45.62
36.26
27.99
25.71
200 190 180 170 160 150 140 130 120 110 100 90 80 70 60 50 40 30 20
f1 (ppm)
O
O
N
H
O

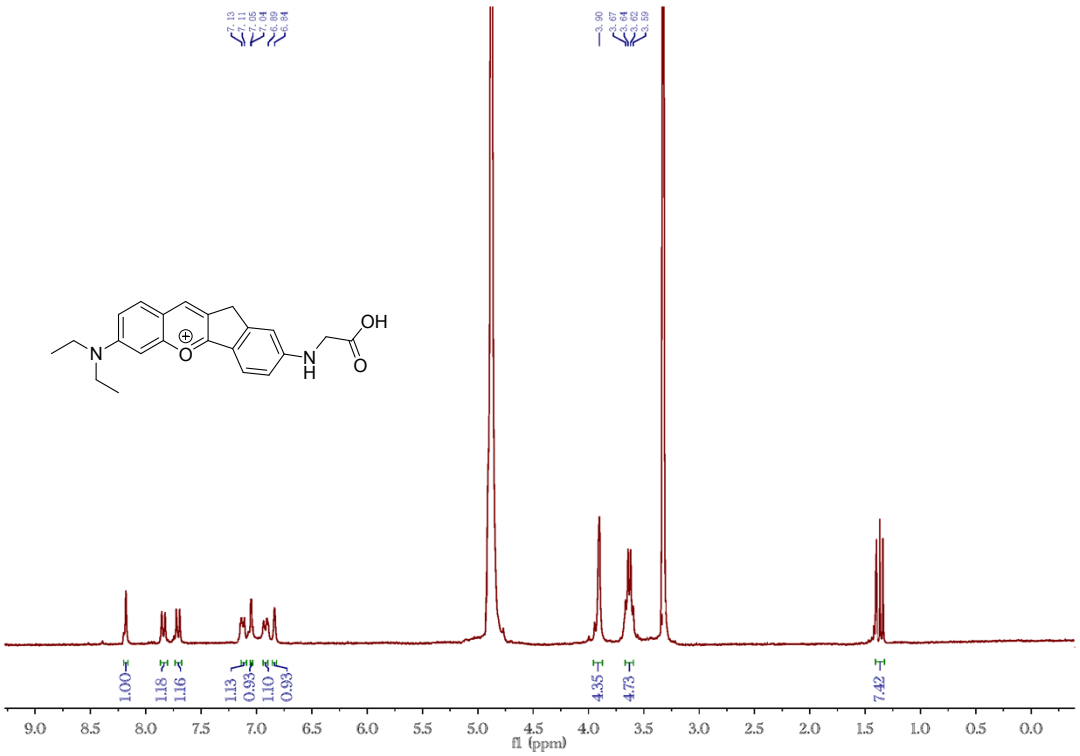
7.13
7.11
7.06
7.04
6.89
6.84
3.90
3.67
3.64
3.62
3.59
OH
N
H
O
1.00
1.18
1.16
1.13
0.93
1.10
0.93
4.35
4.73
7.42
9.0
8.5
8.0
7.5
7.0
6.5
6.0
5.5
5.0
4.5
4.0
3.5
3.0
2.5
2.0
1.5
1.0
0.5
0.0
f1 (ppm)

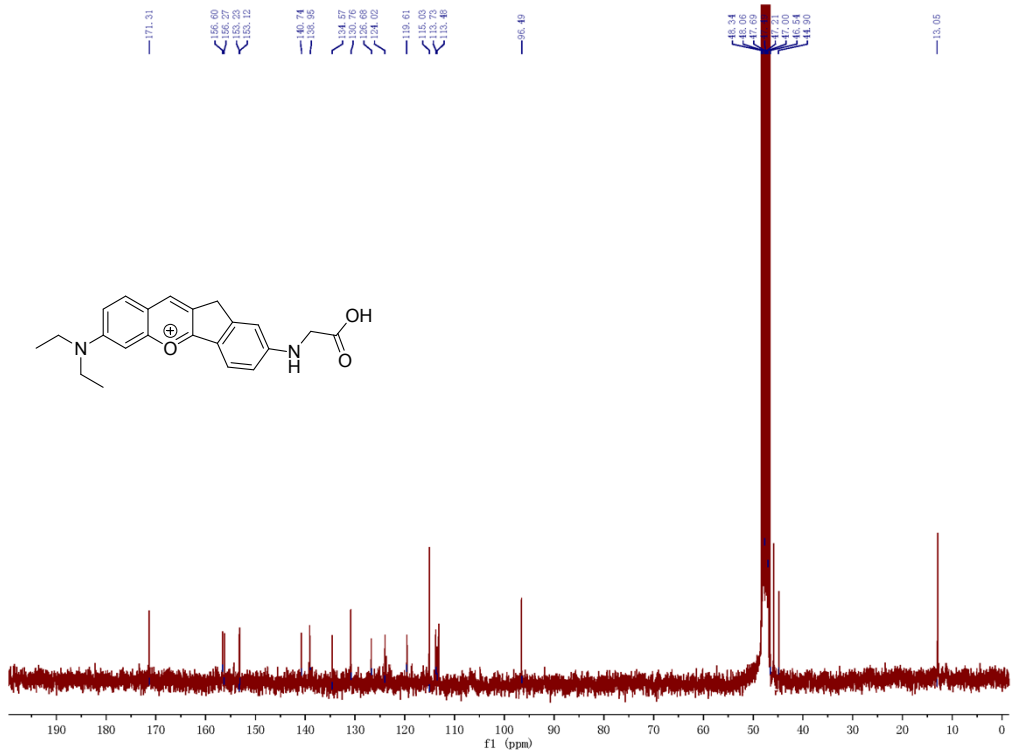
171.31
166.60
166.27
155.29
153.12
140.74
138.95
134.57
130.76
126.69
124.02
119.61
115.03
113.72
113.48
96.49
48.34
48.05
47.69
47.21
47.10
46.87
44.90
13.05
OH
N
H
O
190
180
170
160
150
140
130
120
110
100
90
80
70
60
50
40
30
20
10
0
f1 (ppm)